Pramana – J. Phys. (2016) 87: 100
DOI 10.1007/s12043-016-1305-8

Influence of substrate temperature on certain physical properties and antibacterial activity of nanocrystalline Ag-doped In_2O_3 thin films

P DEEPA and P PHILOMINATHAN*

PG and Research Department of Physics, A.V.V.M. Sri Pushpam College, Poondi 613 503, Thanjavur, India
*Corresponding author. E-mail: philominathan@gmail.com

MS received 16 July 2015; revised 19 November 2015; accepted 18 April 2016; published online 12 November 2016

Abstract. Nanocrystalline Ag-doped indium oxide (AIO) thin films, by employing a much simplified spray pyrolysis technique in different substrate temperatures (300, 350, 400 and 450°C), were fabricated for the first time. The deposited films were subjected to various characterization studies, to explore certain features like the influence of various deposition temperatures on physical and antibacterial properties. XRD results showed that all the samples exhibited preferential orientation along the (2 2 2) plane. The variation in the crystalline size with increasing substrate temperature was explained on the basis of the Zener pinning effect. The electrical sheet resistance (R_{sh}) was found to decrease sharply with increasing substrate temperature and attained a minimum value (62Ω/□) at 400°C and then started increasing for higher deposition temperatures. Further, PL emission spectra of the samples in the visible range ascertained the possibility of applicability of the same in nanoscale optoelectronic devices. From the studies, it was found that at 400°C deposition temperature, one could expect better antibacterial efficiency against *Escherichia coli*. The influence of the shape and size of AIO nanograins on the antibacterial activity was analysed using scanning electron microscopy images.

Keywords. AIO thin films; spray pyrolysis; biological application; electrical properties; scanning electron microscopy; antibacterial activities.

PACS Nos 05.45.−a; 47.52.+j

1. Introduction

The development of cost-effective and highly efficient antibacterial agents is one of the major requirements of medical science. The most common inorganic antibacterial agents include metal oxide semiconductors as they are safe and stable [1,2]. Due to these unique advantages, such antibacterial agents play key roles in a wide range of applications and hence received more recognition in the antibacterial product market [3,4]. Human beings are often infected by microorganisms like bacterium, mold, yeast, virus, etc., in the living environment. Research has been intensive on antibacterial materials containing various natural and inorganic substances such as tea extraction, chitosan, copper, zinc, etc. [5–7]. Among them, silver or silver ions have long been known to have powerful antibacterial activity [8]. Several researchers have tried to explain the inhibitory effect of silver on bacteria. It is generally believed that heavy metals react with proteins by combining the –SH groups of enzymes, leading to the inactivation of proteins as investigated by Feng *et al* [9] and in that report, the inhibition mechanism of silver ions on microorganism was also studied. Silver ions affect DNA molecules that have lost their replication abilities and interact with thiol groups in protein, inducing the inactivation of the bacterial proteins. Therefore, silver has been commercially used to take advantage of its antibacterial properties [10]. Compared to pure silver, silver-doped materials show higher adhesive property. Moreover, silver-doped materials are chemically durable and release silver ions for a long period of time [11]. Silver-doped indium and ceramics are expected to be antibacterial materials, because they are assumed to show high chemical durability and antibacterial activity and these would be satisfied if thin-film technique is adopted. Certain areas like health care zones, hospitals, air and water purifiers require efficient antibacterial materials which can work for larger area and thin films serve the purpose well.

Considering the above aspects, in the present study, we wish to report the results of Ag-doped In_2O_3 (AIO) thin films prepared using a highly economic and effective technique, namely simplified spray pyrolysis. Though there are numerous thin-film fabrication techniques [12–21], the technique adopted in the present investigation offers several advantages such as large deposition area, simple equipment, low fabrication cost, and high homogeneity of the precursor. In earlier reports [22–24], Ag-doped In_2O_3 films were prepared using DC magnetron sputtering technique at a low substrate temperature (300 K) and the properties of the films were studied. The effect of various substrate temperatures (300°C–450°C) on the structural, optical, electrical, photoluminescence and surface morphological properties of AIO thin films along with its antibacterial activity against the bacteria *E. coli* have been investigated in the present work. To the best of our knowledge, this is the first report on the antibacterial activity of silver-doped indium oxide thin film using a low-cost and simplified spray pyrolysis technique. This method is found to be simple, cost-effective and can be used to prepare dense films on large areas with better quality.

2. Experimental details for the preparation of thin films

Silver-doped indium oxide (AIO) thin films were synthesized by a simplified spray pyrolysis technique with fixed concentration ($InCl_3 = 6$ at.% and $AgNO_3 = 2$ at.%) for various substrate temperatures (300°C–450°C). For the preparation of spray solution, the required amount of indium (III) chloride (99.9% from Alfa Aser) was dissolved in a mixture of doubly distilled water and 10 ml of ethanol. Separately, silver nitrate ($AgNO_3$) (99% from Alfa Aser) which is the dopant material, was dissolved in double distilled water and finally both the solutions were mixed together using a magnetic stirrer. Then, the final transparent solution was manually sprayed onto the preheated glass substrate. During spray process, the rate of spray was maintained at 2 ml/min and the substrate was kept 30 cm away from the spray gun (perfume bottle), angle between the nozzle and substrate was fixed at 45° and the time duration of spray deposition was 20–30 min as shown in figure 1 [24]. Hence, the overall reaction process can be described as the thermal decomposition of starting materials in the presence of water and air. The prepared samples were characterized using X-ray diffraction (XRD) patterns obtained from the computer-controlled Philips x-pert PRO XRD system (CuKα radiation; $\lambda = 1.5405$ Å) in Bragg–Brentano geometry ($\theta/2\theta$ coupled). The Joint Committee on Powder Diffraction Standards (JCPDS) database from the International Center for Diffraction Data (ICDD) was utilized for the identification of crystalline phases. The electrical properties were studied using Hall effect apparatus (ECOPIA HMS-3000) with van der Pauw configuration. The surface morphology was recorded by employing scanning electron microscope (HITACHI S-3000H) with xenon lamp (450 W). The photoluminescence spectra of the film at room temperature were recorded using Jobin Y von-FLUROLOG FL3-11. The antibacterial activity against *Escherichia coli* was examined.

2.1 *Culture of Escherichia coli*

Pure culture of *E. coli* species of bacteria was procured from Rontgen Laboratory, India. The microorganisms were identified and confirmed by the microbiologists of the Department of Microbiology, Thanjavur Medical College, Thanjavur. A loop, full of microorganisms, was suspended in about 10 ml of physiological saline in a Roux bottle. *E. coli* which was incubated at 25°C for 24 h was streaked onto the appropriate culture slants incubated at 37°C for 24 h. After the incubation period, when growth was observed, the tubes were kept at 2–8°C until use.

2.2 *Evaluation of antibacterial activity*

Antibiogram was done by disc diffusion method using thin films [25,26]. Petri plates were prepared by pouring 30 ml of nutrient agar medium for bacterial growth. The test organism was inoculated on a solidified agar plate with the help of micropipette and the spreaded part is allowed to dry for 10 min. The surfaces of the media were inoculated with bacteria from a broth culture. A sterile cotton swab dipped into a standardized bacterial test suspension was used to evenly inoculate the entire surface of the nutrient agar plate. Using sterile forceps, thin films were laid down on the nutrient agar plates containing the inoculums of *E. coli*. The plates were incubated at 37°C for 24 h. Each sample was tested in triplicate.

3. Results and discussion

3.1 *Structural studies*

The structural analysis of the prepared samples was carried out by X-ray diffraction spectrometer as depicted in figure 2. The patterns show six well-defined peaks amidst less intense peaks that correspond to

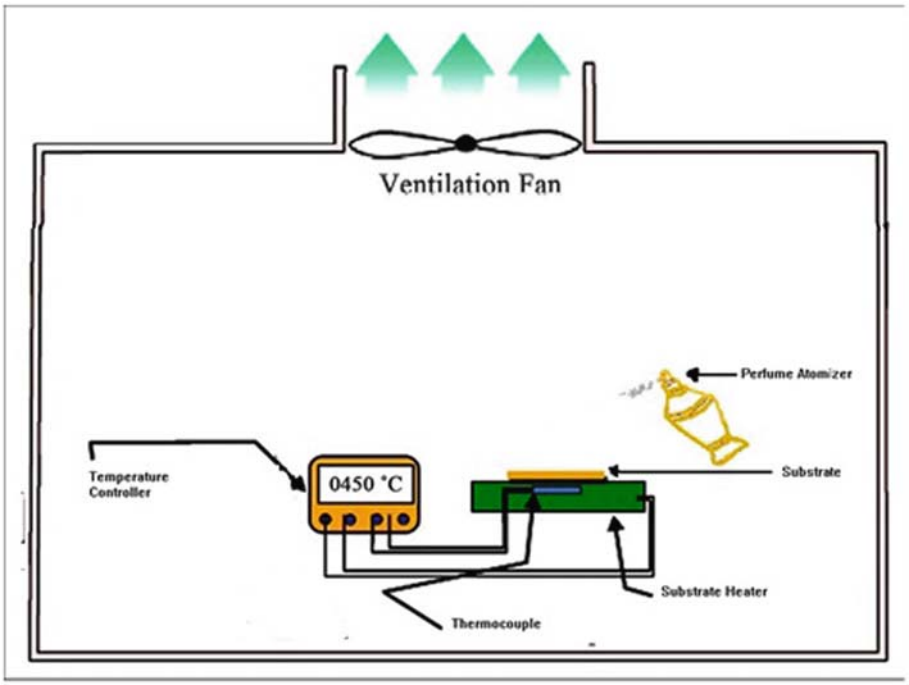

Figure 1. Schematic diagram of the spray pyrolysis unit.

InO phase with a cubic structure (JCPDS No. 00-006-0416). The intensity of the diffraction peaks was slightly increased with substrate temperature, thereafter it got decreased when the substrate temperature approached 450°C as evident from figure 2. The reasons for the less crystallinity of the films are the presence of defects and the lack of enough kinetic energy and mobility of the grains to get oriented at respective planes. The samples prepared at high substrate temperature (450°C) show two additional diffraction peaks, (1 1 1) and (3 2 1), corresponding to the InO phase and for all the samples peaks corresponding to the Ag phase could not be detected. The decrease in the intensity of the peaks for the films prepared at 450°C shows the degradation in crystalline quality which may be attributed to the compression stress arising from the different ionic radii of substituted Ag^{1+} (7.9×10^{-11} m) on In^{3+} (8.1×10^{-11} m) [27]. The average crystalline size was estimated by using the well-known Scherrer's formula [28] and the obtained crystallite size was found to be in the nanorange and the grain size of AIO for various substrate temperatures 300°C, 350°C, 400°C and 450°C are 14, 19, 31 and 24 nm respectively. The crystallite size of the AIO film increases with increase in deposition temperature (at 400°C) and for further increase in the deposition temperature, it gets decreased to 24 nm (at 450°C). The result obtained can be interpreted using Zener pinning effect [29]. The outward movement (expansion) of grain boundaries is restricted by the retarding force generated by crystal imperfections like vacancies and interstitials. In the present investigation, the number of oxygen vacancies present in the InO lattice may be large only when Ag is doped with InO. These oxygen vacancies restrict the growth of crystallites due to the Zener pinning effect. But, when the substrate temperature increases, these oxygen vacancies may be filled by the incorporated In ions. Therefore, the influence of retarding force decreases gradually, allowing the crystallites to grow larger in size. This trend is followed upto the film deposition temperature 400°C and thereafter the crystalline size decreases as the excess In ions incorporated in the lattice are positioned as interstitials which may again enhance the retarding force causing Zener pinning effect.

3.2 *Electrical properties*

The variation in electrical sheet resistance (R_{sh}) of the silver-doped indium oxide thin film as a function of various deposition temperatures is shown in figure 3. R_{sh} decreases sharply as the deposition temperature increases, attaining a minimum value ($62\Omega/\square$) at 400°C and then increases for further increase in the substrate temperature. This variation in R_{sh} can be explained as follows: The initial decrease in R_{sh} is caused by the substitution of In^{3+} ions into the Ag^{1+} sites, because each of this substitution results in the creation of two free electrons. In other words, the substituted In^{3+} ions act as donors to the system

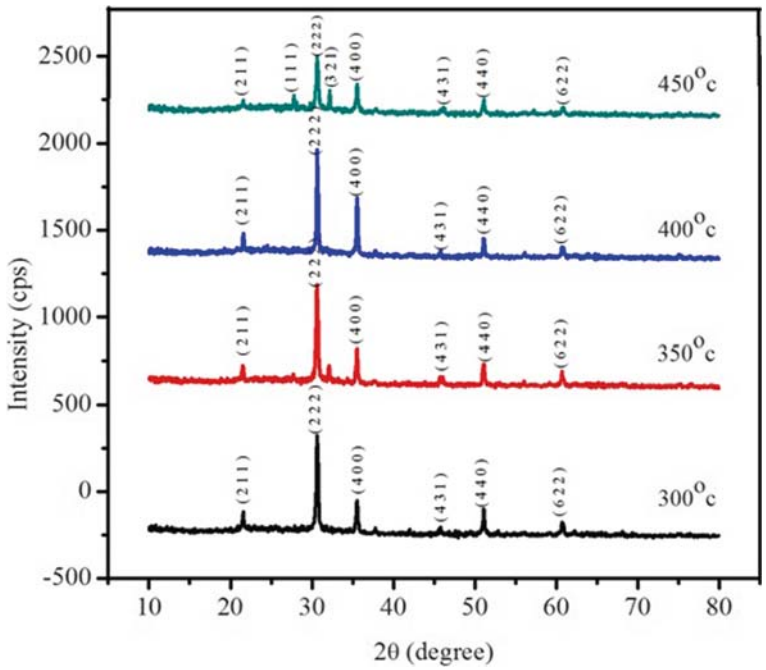

Figure 2. XRD patterns of Ag-doped indium oxide thin film as functions of different deposition temperatures.

thus reducing R_{sh}. This trend is valid upto a certain deposition level only (in this study, it is 400°C), and beyond 400°C the In^{3+} ions got reduced to Ag^{1+} state by absorbing the pair of electrons already available in the system, thereby causing a reduction in the number of free carriers which in turn increases R_{sh}. The film deposited at 400°C has the minimum value of sheet resistance (62Ω/□) and it possess the best antibacterial activity [30] and the results are confirmed in §3.5. This inference from the obtained electrical result is derived on the basis of one of the important characteristic features of the p-block elements as discussed below: the p-block elements of the periodic table having higher atomic number, have lesser tendency to use *s* electrons for chemical bonding and hence they are stable only in the lower oxidation states. Hence, we strongly believe that beyond 400°C, the In^{3+} ions are reduced to the Ag^{1+} state by absorbing a pair of electrons in the vicinity. It is reasonable to assume that the reduction process can start only when the number of free electrons available in the system is sufficiently high to initiate this phenomenon and the film deposited at 400°C reached this stage and Vaezi and Sadnezhaad [31] reported the possible mechanism related to the variation in R_{sh}.

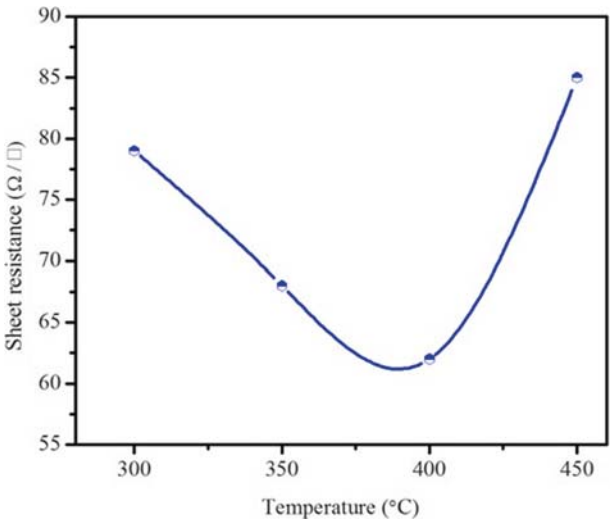

Figure 3. Variation in electrical sheet resistance (R_{sh}) of silver-doped indium oxide thin films as functions of substrate temperatures.

3.3 *Photoluminescence studies*

Photoluminescence spectroscopy is a powerful tool to study the optical quality of semiconductor materials. The spectral positions and the corresponding intensities of PL emission peaks can be used for the identification of defects and their concentrations, respectively. Room-temperature photoluminescence (PL) studies were carried out for silver-doped indium oxide thin films with three distinct excitation wavelengths and their spectra are depicted in figure 4. It can be seen that when the films were excited with 350 nm radiation, a single high intensity peak was found at 628 nm and three low-intensity peaks were obtained around 394, 412 and 573 nm. When the samples were excited with 450 nm radiation, the PL emission peaks

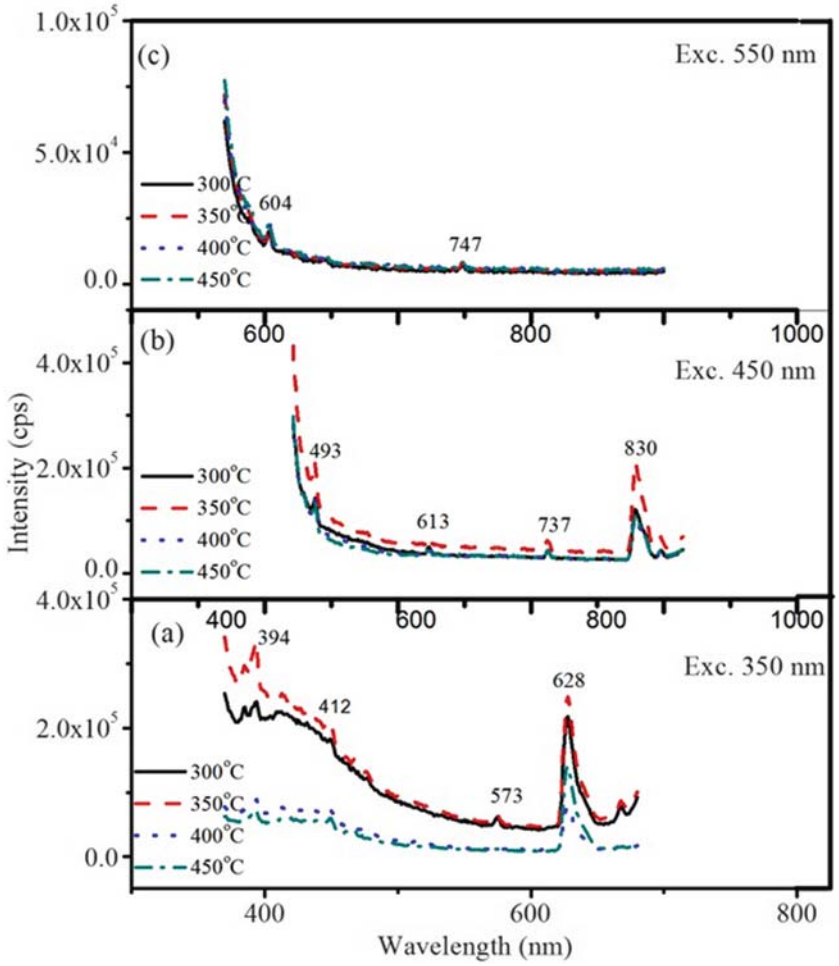

Figure 4. Photoluminescence spectra of AIO thin films with three distinct excitation wavelengths (**a**) 350 nm, (**b**) 450 nm, (**c**) 550 nm.

were found to occur at 493, 613, 737 and 830 nm. Finally, when the films were excited with 550 nm radiation, only a few low-intensity peaks at 604 nm and 747 nm were found. As the excitation wavelength increased from 350 nm to 550 nm, the intensity of emission peaks got decreased and more number of prominent peaks were found to emerge in the visible region and then got diminished. The emergence of low-intensity peaks of these samples may be due to the interimpurity transitions and larger stoichiometric deviation. The PL emission located at 493 nm was originated from the direct recombination of electron/hole pairs and emission at 412 nm was due to the oxygen vacancy trapping (F+ centre), that is the generation of charged oxygen vacancy defects. It is evident that when the number of charge defects in samples are more, more O_2 will be adsorbed to the sample by electrostatic forces. Meanwhile, the electrons trapped at the charged oxygen-vacancy defects may be transferred to the adsorbed O_2 to form superoxide species. Therefore, the emission at 412 nm comes from the F+ centre, which is referred to as oxygen vacancies trapping an electron. Moreover, the well-defined UV emission centred at 394 nm was observed for all samples and this emission can be ascribed to the nearest band-edge transition wherein photogenerated holes near the valence band recombine with electrons in the donor levels through a radiative process [32–34]. The PL emission at 573 nm (yellow emission) is due to $^4F_{6/2} \rightarrow {}^6H_{13/2}$ transitions and high intense red emission was found at around 628 nm and other weak intensity peaks were found centred at 737 and 747 nm which can be attributed to the zero-phonon, PL line and its two vibronic progressions respectively. Although the PL emission mechanism of indium oxide is not very clear so far, it has been recognized that the oxygen vacancies act as donors and induce PL emission under photon excitation. Hence, well-defined emission peaks were found when the excitation wavelength is in the range of 350–450 nm and

as the excitation wavelength approaches 550 nm, the intensity of PL emission decreases and the PL emission is found to be constant, irrespective of the intensity as evident from figure 4. The less intense emissions obtained for all samples indicate the lesser defect concentration of these films. The shift in UV peak (films excited with 350 nm) towards lower wavelength side (blue-shift) increases along with deposition temperature upto 350°C indicating the enhancement of radiative recombination centres due to the substitution of In^{3+} ions into Ag^{1+} sites as discussed in electrical studies (§3.2). At the same time, the reduction in UV intensity for films deposited at (400°C and 450°C) AIO thin films, indium attributed to the introduction of defects responsible for non-radiative transition. The PL light emitting property in the UV region at room temperature suggests the possible applications of these films from nanoscale to electronic devices in future. The absence of PL intensity peak at 628 nm with an excitation wavelength of 550 nm, was due to the significantly higher defect density [35]. For the films excited with 350 nm, the strongest peaks at 412 and 573 nm are assigned to the transition of electrons from In_i levels to the valence band [36] and the peaks at 394 and 628 nm arise due to the presence of singly ionized oxygen vacancies in InO. These singly ionized oxygen vacancies generally act as the origin for the generation of OH^- ions on the surface when AIO is used as an antibacterial agent [37]. These OH^- ions play key roles in improving the efficiency of antibacterial agents which will be discussed in the forthcoming section.

3.4 *Surface morphological studies*

The SEM images of AIO thin film as a function of different substrate temperatures (300, 350, 400 and 450°C) are shown in figure 5. The surface morphologies of all the samples show a closely packed arrangement of particles and it can be seen that the morphology changes with substrate temperature. From figure 5, the spherical grains of 82, 89, 90 and 60 nm sizes for the films deposited at various temperatures (300, 350, 400 and 450°C) can be visualized. Increasing substrate temperature causes remarkable changes in the shape and size of the particles and with further increase in deposition temperature (450°C), the particle size decreases (60 nm) as shown in figure 5. The slightly larger sized particles more readily enables them to penetrate and interact with the interior of the bacteria thereby destroying it [38]. The antibacterial efficiency of the films gets enhanced with increasing substrate temperature upto 400°C as discussed in §3.5. If the deposition temperature is further increased (450°C), the particles attain irregular shapes with varying sizes. The change in the surface morphology may be ascribed to the presence of more number of Ag interstitial defects leading to a deformation in the InO lattice.

3.5 *Antibacterial studies*

The antibacterial activity of AIO thin film with different substrate temperatures (300, 350, 400 and 450°C) was investigated against *E. coli* using disc diffusion method as shown in figures 6a–6d. The presence of remarkable inhibition zones indicates the better

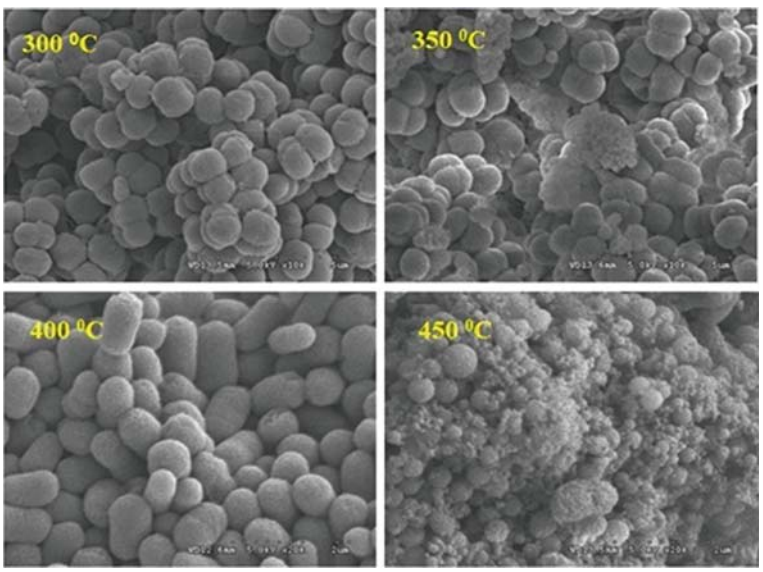

Figure 5. SEM images of AIO thin film as functions of different substrate temperatures.

antibacterial efficiency of samples against the microorganisms. From figures 6a–6d, it is observed that AIO samples prevented the growth of bacteria remarkably and formed well-defined zones around the samples and the zone of inhibition increases with an increase in the deposition temperature. For comparison, the variation in the diameter of the zone of inhibition is plotted against different substrate temperatures (300, 350, 400 and 450°C) and is presented as a bar diagram in figure 7. The antibacterial activity of the AIO thin film may be related to several mechanisms, including the generation of reactive oxygen species (ROS) and RNS production mechanisms have been thoroughly investigated and can be classified into three groups: intrinsic production, produced by the interaction with cellular targets, and production mediated by the inflammatory reaction. The three groups share responsibility for most of the genotoxic effects so far observed in nanoparticles. The factors responsible for antibacterial activity of AIO are: (i) release of Ag^{1+} ions, (ii) generation of reactive oxygen species (ROS) and (iii) reduced size of the grains. These three factors may lead to the rupture of the cellular contents and subsequent cell death [39]. The mechanism of the antibacterial activity of Ag-doped InO thin films can be explained as follows: When Ag is doped with InO, the substitutional incorporation of Ag^{1+} ions into In^{3+} sites allows more In^{3+} ions to occupy the interstitial positions of an InO matrix as the ionic radii of Ag^{1+} (7.9×10^{-11} m) is remarkably higher than that of In^{3+} (8.1×10^{-11} m). This result supports the discussion given in the structural studies. As In^{3+} ions in the interstitial positions can be released easily from the lattice when compared with those in regular sites, this AIO has high potential to act as better antibacterial agent. They released In^{3+} ions which can directly diffuse into cell membranes, causing severe damage to the cell wall and the subsequent leakage of cell contents. The diffusion of In^{3+} ions from the AIO thin film into the food stuff, drinking water, etc. cannot cause any harmful effect on humans

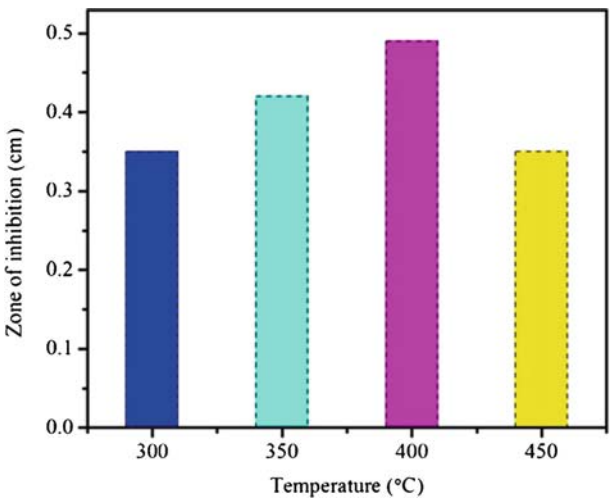

Figure 7. Variation in the zone of inhibition as a function of different substrate temperatures.

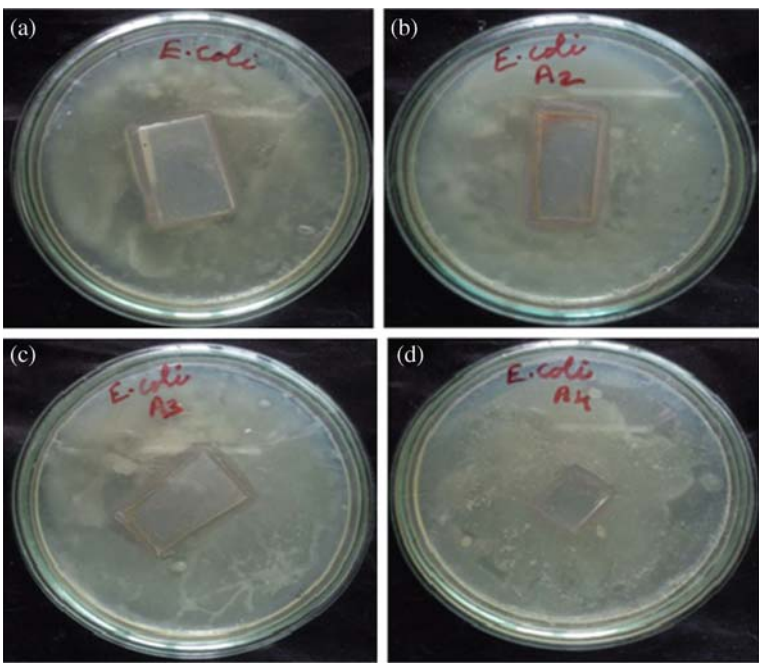

Figure 6. Zone of inhibition of AIO thin films under substrate temperature: (**a**) 300°C, (**b**) 350°C, (**c**) 400°C and (**d**) 450°C.

as Ag is an effective nutrient [40]. From figure 7, it is evident that the antibacterial activity of AIO thin films increases with increasing deposition temperature up to 400°C and then decreases for further increase in the substrate temperature. This increase in antibacterial activity of AIO up to 400°C may be due to the creation of a large number of free electrons which caused the substitution incorporation of Ag^{1+} ions from InO lattice and on coming in contact with bacterial cells can produce reactive oxygen species (ROS) such as hydroxyl radicals, superoxide and H_2O_2 [41,42]. But, when the substrate temperature increases further (450°C), the excess Ag^{1+} ions begin to occupy the interstitial sites of InO matrix leading to a decrease in the number of free electrons. This may be the reason for the decrease in the zone of inhibition of AIO thin films beyond 400°C. The generation of ROS can be represented as follows [43]:

$$\mathrm{InO} + h\nu \rightarrow h^+ + e^-, \quad (1)$$

$$h^+ + \mathrm{H_2O} \rightarrow \mathrm{OH^{\cdot}} + \mathrm{H^+}, \quad (2)$$

$$\mathrm{O_2} + e^- \rightarrow \mathrm{O_2^{\cdot -}}, \quad (3)$$

$$\mathrm{O_2^{\cdot}} + \mathrm{H^+} \rightarrow \mathrm{HO_2^{\cdot}}, \quad (4)$$

$$\mathrm{H^+} + \mathrm{HO_2^{\cdot}} + e^- \rightarrow \mathrm{H_2O_2}, \quad (5)$$

$$\mathrm{H_2O_2} + \mathrm{O_2^{\cdot -}} \rightarrow \mathrm{OH^{\cdot}} + \mathrm{O_2} + \mathrm{OH^-}. \quad (6)$$

From these reactions, it is seen that, the electron–hole pairs play vital roles in the generation of ROS. Among the ROS, H_2O_2 is a more powerful oxidizing agent and it directly penetrates into the cell membrane of the bacteria, causes various types of injuries and prevents the growth of the cells, whereas, the negatively charged hydroxyl radicals and superoxide anions cannot penetrate into the cell membrane, but they can cause severe damage to proteins, lipids, DNA and profiles of the outer wall of the bacteria [44], thereby leading to the destruction of the bacteria. In addition, in our present work, particle size increases with deposition temperature upto 400°C and a further increase in temperature (450°C) decreases the particle size as evident from SEM results. Thus, the size of the particle plays a crucial role in improving the antibacterial activity of the AIO thin films.

4. Conclusion

Good-quality nanocrystalline AIO films were deposited using the simplified spray pyrolysis technique and the effects of substrate temperatures (300, 350, 400 and 450°C) on certain physical properties and antibacterial activity were studied. The sample deposited at 400°C exhibit highest antibacterial efficiency against *E. coli*. The structural studies revealed that all the films exhibit cubic structure with preferential orientation along the (2 2 2) plane. The observed variation in the electrical sheet resistance (R_{sh}) induced by different substrate temperatures, was clearly explained on the basis of the important characteristic features of p-block elements. All the films exhibit intense PL emission in the UV region. The size of the particle also has a remarkable impact on the antibacterial efficiency as observed from SEM studies. The antibacterial studies revealed that the film deposited at 400°C is most suitable for antibacterial activities of AIO films.

References

[1] K Krishnamoorthy, M Veerapandian, L H Zhang, K Yun and S J Kim, *J. Phys. Chem.* **116**, 17280 (2012)
[2] M Fang, J H Chen, X L Xu, P H Yang and H F Hildebrand, *Int. J. Antimicrob. Agents* **27**, 513 (2006)
[3] X J Wang, X L Qiao, J G Chen, H S Wang and S Y Ding, *J. Ceram.* **24**, 239 (2003)
[4] Y Xu, Z X Yang, Z H Li, J M Qian and Z W Shen, *J. Funct. Mater.* **33**, 682 (2002)
[5] S G Yeo, C H Ahn, I S Kim, Y B Park, Y H Park, S B Kim and J Korean, *J. Korean Soc. Food Nutr.* **24**, 293 (1981)
[6] B O Jung, Y M Lee, J J Kim, Y J Choi, K J Jung and S J Chung, *Ind. Eng. Chem.* **10**, 660 (1999)
[7] T N Kim, Q L Feng, J O Kim, J Wu, H Wang, G C Chen and F Z Cui, *J. Mater. Sci.: Mater. Med.* **9**, 129 (1998)
[8] H Y Kang, M J Jung and Y K Jeong, *Biotechnol. Bioeng.* **15**, 521 (2000)
[9] Q L Feng, J Wu, G Q Chen, F Z Cui, T N Kim and J O Kim, *J. Biomed. Mater. Res.* **52**, 662 (2000)
[10] M Kawashita, S Tsuneyama, F Miyaji, T Kokubo, H Kozuka and K Yamamoto, *Biomaterials* **21**, 393 (2000)
[11] T Toshikazu, *Inorganic Mater.* **6**, 505 (1999)
[12] J Nishino, T Kawarada, S Ohshio, H Saitoh, K Maruyama and K Kamata, *J. Mater. Sci. Lett.* **16**, 629 (1997)
[13] N F Cooray, K Kushiya, A Fujimaki, I Sugiyama, T Miura, D Okumura, M Sato, M Ooshita and O Yamase, *Sol. Energy Mater. Sol. Cells* **49**, 291 (1997)
[14] O Kluth, G Schope, B Rech, R Menner, M Oertel, K Orgassa and H W Schock, *Thin Solid Films* **502**, 311 (2006)
[15] A Kuroyanagi, *Jpn J. Appl. Phys.* **28**, 219 (1989)
[16] R Groenen, J L Linden, H R M van Lierop, D C Schram, A D Kuypers and M C M van de Sanden, *Appl. Surf. Sci.* **173**, 40 (2001)
[17] E S Sub, H S Kang, J S Kang, J H Kim and S Y Lee, *Appl. Surf. Sci.* **186**, 474 (2002)
[18] Z Fu, B Lin and J Zu, *Thin Solid Films* **402**, 302 (2002)
[19] P Nunes, B Fernandes, E Fortunato, P Vilarinho and R Martins, *Thin Solid Films* **337**, 176 (1999)
[20] W Tang and D C Cameron, *Thin Solid Films* **238**, 83 (1994)
[21] N Balaguru and P Philominathan, *Int. J. Renewable Energy Technol. Res.* **2**, 196 (2013)
[22] A Subrahmanyam and Ullash Kumar Barik, *J. Phys. Chem. Solids* **67**, 1518 (2006)
[23] Ullash Kumar Barik, S Srinivasan, C L Nagendra and A Subrahmanyam, *Thin Solid Films* **429**, 129 (2003)

[24] A Subrahmanyam and U K Barik, *Appl. Phys. A* **84**, 221 (2006)
[25] NCCLS-(1993) National Committee for Clinical Laboratory Standards, *Performance standards for antimicrobial disc susceptibility tests. PA: NCCLS Publications*, **-**, p. M2-A5 (1993)
[26] O Awoyinka, I O Balogun and A A Ogunnowo, *J. Med. Plant* **3**, 63 (2007)
[27] D Beena, R Vinodkumar, I Navas, V Ganasen, A Yamuna and V P Mahadevan Pillai, *J. Alloys Compds.* **539**, 63 (2012)
[28] Buerger Azaroff, *Powder method in X-ray crystallography* (McGraw-Hill Publishers, New York, 1958)
[29] N Moelans, B Blanpain and P Wollants, *Acta Mater.* **55**, 2173 (2007)
[30] J Sawai, *J. Microbiol. Methods* **54**, 177 (2003)
[31] M R Vaezi and S K Sadrnezhaad, *Mater. Sci. Eng. B* **141**, 23 (2007)
[32] H Cao, X Qiu, Y Liang and Q Zhu, *Appl. Phys. Lett.* **83**, 761 (2003)
[33] C J Chen, W L Xu and Y Chern, *Adv. Mater.* **19**, 3012 (2007)
[34] Z P Wei, D L Guo, B Liu, R Chen, L M Wong, W F Yang, S J Wang, H D Sun and T Wu, *Appl. Phys. Lett.* **96**, 031902 (2010)
[35] Tanya Paskova, *Nitrides with nonpolar surface growth, properties and devices* (John Wiley & Sons, 2008) Vol. 1
[36] P Suresh Kumar, P Paik, A Dhayal Raj, D Mangalaraj, D Nataraj, A Gedanken and S Ramakrishna, *Appl. Surf. Sci.* **258**, 6765 (2012)
[37] L V Trandafilovic, D K Bozanic, S Dimitrijevic-Brankovic, A S Luyt and V Djokovic, *Carbohydr. Polym.* **88**, 263 (2012)
[38] Aruna Jyothi Kora and R B Sashidhar, *Arab. J. Chem.*, DOI:10.1016/j.arabjc.2014.10.036 (2014)
[39] Ishita Matai, Abhay Sachdev, Poornima Dubey, S Uday Kumar, Bharat Bhushan and P Gopinath, *Colloids Surf. B: Biointerfaces* **115**, 359 (2014)
[40] D Dellasega, A Facibeni, F Di Fonzo, M Bogana, A Polissi, C Casari, A Li Bassi and C E Bottani, *Nanotechnol.* **19**, 475 (2008)
[41] R Tankhiwale and S K Bajpai, *Colloids Surf. B: Biointerfaces* **90**, 1620 (2012)
[42] R Kohen and A Nyska, *Toxicol. Pathol.* **30**, 620 (2002)
[43] A Neal, *Ecotoxicol.* **17**, 362 (2008)
[44] Yang Li, Wen Zhang, Junfeng Niu and Young Sheng, *NCS Nano.* **6**, 5164 (2012)